

Contents lists available at [ScienceDirect](http://www.sciencedirect.com)

Optics Communications

journal homepage: www.elsevier.com/locate/optcom

Development of targeted STORM for super resolution imaging of biological samples using digital micro-mirror device

Liyana Valiya Peedikakkal^a, Victoria Steventon^b, Andrew Furley^b, Ashley J. Cadby^{a,*}^a The Department of Physics and Astronomy, Hicks Building, Hounsfield Road, Sheffield S3 7RH, United Kingdom^b The Bateson Centre and Department of Biomedical Science, University of Sheffield, Sheffield S10 2TN, United Kingdom

ARTICLE INFO

Keywords:

Localization microscopy
Digital mirror device
Super-resolution
STORM

ABSTRACT

We demonstrate a simple illumination system based on a digital mirror device which allows for fine control over the power and pattern of illumination. We apply this to localization microscopy (LM), specifically stochastic optical reconstruction microscopy (STORM). Using this targeted STORM, we were able to image a selected area of a labelled cell without causing photo-damage to the surrounding areas of the cell.

© 2017 The Authors. Published by Elsevier B.V. This is an open access article under the CC BY-NC-ND license (<http://creativecommons.org/licenses/by-nc-nd/4.0/>).

1. Introduction

In recent years, the Abbe limit restricting the resolution of optical systems to the diffraction limit has been overcome [1]. There have now been many independent solutions to this century old puzzle and these include, but are not limited to, Structured Illumination Microscopy (SIM) [2,3], Stimulated Emission Depletion Microscopy (STED) [4] and, Localization microscopy (LM) [5,6]. In LM the inherent relative stabilities of the optical bright and dark states within a molecule are tuned to allow only a small subset of the molecules under study to be optically active at any point in time. This is then used to reduce the density of emitting molecules to the point where each emitting molecule is separated by a distance greater than the diffraction limit, essentially making the single molecule resolvable.

By fitting the corresponding image of each emitting molecule to the point spread function (PSF) of the optical system the location of the molecule can be determined to within a few nanometres [7]. The emitting molecules are then returned to their dark state or a bleached state and a different subset of molecules are activated. This process is repeated until a substantial number of single molecules have been localized. The localizations are used to build a molecular map with nanometre resolution of all the molecules of interest.

LM along with the other techniques mentioned above have begun to provide novel insights into biological systems [8]. However, in general the increase in resolution comes with an increase of photo-toxicity, for example LM, which has the highest resolution of the techniques requires very high laser power densities in the order of 15 kW cm^{-2} . The increase

in optical power has significant problems for imaging live cells due to increased photo-damage [9].

To follow the time progression of biological process using LM researchers have used a variety of methods to follow natural processes in living system, an elegant example is the work by Holden et al. [10]. In that work, they developed a high throughput LM microscope which imaged hundreds of bacteria per super resolution frame, with each frame recorded at a different sample location. Furthermore, each frame was synchronized to the life cycle of the bacteria under observation. This allowed them to image over time the nanoscale organization of the bacterial cell division protein FtsZ in a live system. While this work was incredibly useful at allowing LM to follow growth progression in a synchronized culture where changes over time in different cells can be assumed to represent the changes that also are occurring with a single cell, it is difficult to apply this technique to look at changes occurring within a single cell over time since continued imaging of the whole cell results in cell damage or death.

As a large amount of power is needed for LM microscopy it would be ideal to identify a region of interest, such as single bacteria or a sub region of a eukaryotic cell and during an experiment locally image the region of interest (ROI) using a super-resolution technique, while leaving the surrounding regions unperturbed. This requires a great deal of control from the illumination system used in the imaging platform. There are several ways to control the power delivered to a sample with the most common used in microscopy being a spatial light modulator (SLM) which is generally either a liquid crystal based device which modulates the phase [11] of the signal or a digital mirror device (DMD) which allows an ON/OFF modulation [12].

* Corresponding author.

E-mail address: a.cadby@sheffield.ac.uk (A.J. Cadby).

<http://dx.doi.org/10.1016/j.optcom.2017.06.055>

Received 17 March 2017; Received in revised form 21 May 2017; Accepted 15 June 2017

Available online xxxx

0030-4018/© 2017 The Authors. Published by Elsevier B.V. This is an open access article under the CC BY-NC-ND license (<http://creativecommons.org/licenses/by-nc-nd/4.0/>).

Using SLMs such as twisted nematic or ferroelectric Liquid Crystal on Silicon (LCoS) and DMD, the user can achieve precise control over the illumination pattern and intensity, also, enabling selective light detection from specimen. Although these varieties of available SLMs are quite similar in their function to projecting patterned light onto the sample, the DMD may be considered to be more advantageous, for controlling power delivered to a sample, when compared to its counterparts because of higher contrast ratio, larger spectral range and, higher speed. The DMD allows us to control programmably the source and the detection aperture in 2D to achieve the best signal. In this work we use a DMD based laser illumination system to deliver the high power densities to specific areas of the sample plane of a LM microscope.

2. Experimental setup

A DMD device consists of an array of mirrors which can be switched between two states, in the DMD used in this work, one state sets a mirror at $+12^\circ$ to the normal axis of the DMD chip and one state sets the mirror to -12° to the normal. This allows light incident on a mirror to be reflected at either $+12^\circ$ or -12° . For the rest of this work we defined the $+12^\circ$ state as being 'ON' and the -12° state as being the 'OFF' state.

The illumination system used in the work is based on the dual path programmable array microscope (PAM) by Heintzmann et al. [13] as shown in Fig. 1. This optical design allows us to define an 'ON' and 'OFF' path with each path being associated with a camera and illumination source. Light from the illumination source on the 'ON' side is directed by 'ON' pixels on the DMD towards the image plane of the microscope while 'OFF' pixels on the DMD direct light from this path to a beam stop. In contrast, light from the 'OFF' side is directed to the microscope by 'OFF' DMD pixels while 'ON' pixels are sent to a beam stop.

In this work a Texas Instruments DLP7000 [14] DMD chip controlled through a ViALUX controller board [15] was programmed using Matlab [16]. The combination of these elements allows us to display 1 bit 1024 by 768 pixel images at frame rates of roughly 23 kHz and 8 bit greyscale frames at 300 Hz [15]. In a 1 bit image each pixel is defined as 'ON' or 'OFF' as described above. For 8 bit images the DMD works as a pulse width (PWM) based optical modulator and allowing us to change the amount of power delivered to the sample, with the PWM 'ON' time of each mirror being defined by a value between 0 and 255, with 0 being 100% 'OFF' and 255 being 100% 'ON'.

A Nikon Ti-E inverted microscope was used as the base for the system and the illumination system focused the DMD image plane at the external focal plane of the microscope. Images projected at this plane are then relayed to the sample via the objective lens which de-magnifies the image by the combination of the tube lens and the microscope's objective lens. In this work, the objective lens used was a Nikon 100x ApoTIRF oil objective. The fluorescence, collected by the objective lens, from the sample was then directed back along the original illumination path and collected using one of the cameras. Light from the 'ON' and 'OFF' paths was collected by two Andor Zyla CMOS cameras, one on each path. Using a low pass dichroic filter before the objective it was possible to illuminate the sample with light from the DMD and collect the light from the sample on the back port of the microscope, i.e. negating the return path via the DMD. Light collected at the back port of the microscope was imaged using an Andor EMCCD iXon. Here it is worth noting that the fluorescence from sample because of light projected using the 'ON' path will be imaged using the 'ON' camera, 'OFF' pixels will direct fluorescence towards the 'OFF' camera, such that the 'ON' camera will only contain fluorescence from the 'ON' pattern projected onto the sample.

For example, in Fig. 1 an image of a heart is displayed on the DMD light from the illumination source in the ON path projects an image of the heart on to the sample plane of the microscope. Fig. 1(B) shows the image recorded by the camera on the ON path. This is light collected from the sample which is reflected off the DMD and collected by the ON camera. It should be noted that the image on the DMD acts as a spatial

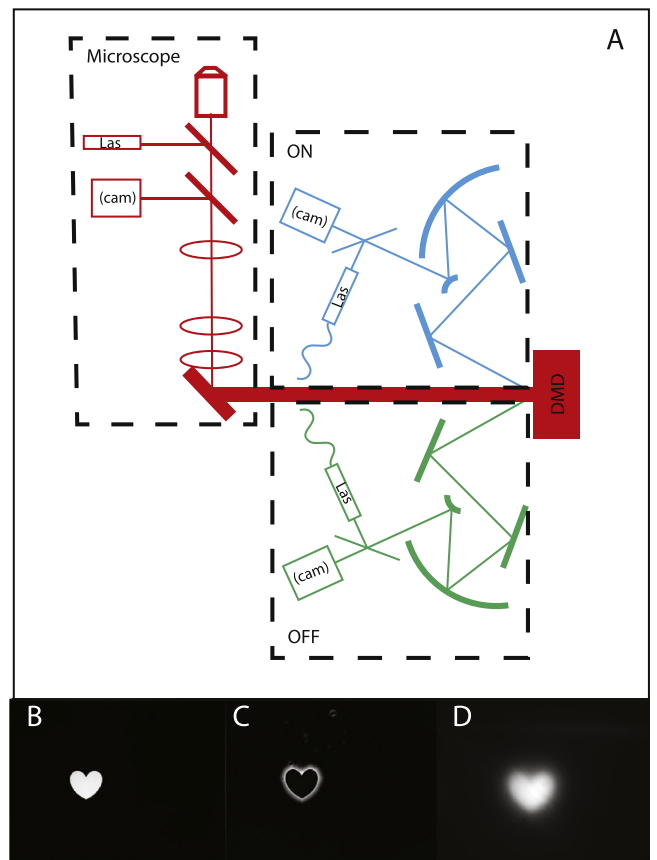


Fig. 1. (A) The optical path for the DMD based illumination system. The ON (blue) and OFF (green) channels, are at $+12^\circ$ and -12° to the DMD, each path way contains both an illumination source and a camera. The red path way depicts the optical path from the DMD to the sample, this pathway also contains a camera (cam) and illumination source (Las) which can be either a laser or LED system. As an example, if the ON path light source is turned on and a image is displayed on the DMD, for example a heart, an image is projected through the illumination optics on to the sample plane of the microscope. Fig. 1 B, C, and D shows the images collected on the ON, OFF an backport cameras respectively. (For interpretation of the references to colour in this figure legend, the reader is referred to the web version of this article.)

filter on the return path. As the DMD acts as a spatial filter only light hitting the DMD's OFF pixels is collected by the OFF camera. Because the light hitting the sample comes from the ON path only out of focus or scattered light is detected on the OFF camera. Fig. 1(C) shows the image collected by the camera on the OFF path, it shows the out of focus light from the sample being illuminated. The patterned illuminated at the sample plane is collected by the camera on the back port of the microscope and is given in Fig. 1(D).

NIH 3T3 cells were grown in standard conditions (10% Fetal Bovine Serum in DMEM + Penicillin-Streptomycin on tissue culture dishes at 37°C). For transfection, 5×10^4 cells/well were plated onto 13 mm cover slips in 24 well plates and incubated overnight before of NrCAM-HA plasmid [17] was introduced using Lipofectamine-2000 (11668019, Invitrogen) according to suppliers' recommendations. The cells were fixed the following day (after 18–24 h at 37°C) using 4% Paraformaldehyde (PFA) in 0.1M phosphate buffer at pH7. Immunolabelling was performed as described [18] NrCAM tagged with HA was detected by anti-HA rat monoclonal (11867423001, Sigma Aldrich; 1:1000 in PBS, 0.05%TX100, 3% normal goat serum (PBST/NGS), incubated overnight at 4°C), which in turn was detected by Alexa Fluor 647 Goat Anti-Rat IgG (A21247-Thermo Fisher Scientific) secondary antibody (1:200 in PBST/NGS, incubated 1–2 h in dark at room temp). Antibody solution was removed and the cells were washed in PBST for 3 washes of 20 min. Coverslips were mounted on microscope slides using STORM buffer

(below) and imaged immediately. For STORM imaging, coverslips need to be mounted over 2 or 3 drops of STORM buffer. STORM buffer for this study is prepared by mixing 100 millimolar monoethanolamine (MEA), 0.5 mg/ml glucosidase, 40 $\mu\text{g/ml}$ catalase and 10% w/v glucose in PBS solution [19].

As previously mentioned STORM requires individual molecules to be isolated, this is achieved by placing most dye molecules in to a dark state, this requires high illumination densities. As such the illumination source for STORM measurements requires a high-power light source, the power of the laser must cover a significant area of the DMD, as such a 7 W multi line laser from Cairn-Research was used. Up to 4 W of 635–645 nm light from the laser was focused on a 400 μm optical fibre, the light emitted from the opposite end of the fibre was collimated to give a 4 mm diameter circular illumination spot which was projected on to the DMD. The laser light was delivered to the DMD via the ON optical path as discussed above. The 4 mm laser spot does not completely cover the DMD, although this limited the area of the DMD that could be used this still covered 75 000 pixels and allowed us a higher power density at the sample. The 4 mm diameter laser spot once projected onto the sample through a 100 \times Nikon SR lens produced a 40 μm diameter spot. Once the area of the DMD containing the laser spot had been identified, it was possible to build a series of images which could be used to illuminate the sample. These patterns could be single value bitmaps used to control the laser power delivered to the sample, for example to allow us to easily switch between a lower power mode for selecting sections of the sample of interest (epifluorescence) or high power for performing localization microscopy. However, the patterns could also be more complicated allowing different sections of the sample to be illuminated with different laser powers. Each pixel on the DMD is 13 μm^2 , after being de-magnified on to the sample by the microscope, this would be 130 nm in size being smaller than the diffraction limit the resulting spot would be equivalent to the point spread function of the microscope. For targeting power to the sample, we can excite the sample from any DMD pixel meaning that we can illuminate any feature down to the diffraction limit of the microscope. In this work, the limiting factor in the maximum size was the area of the laser spot on the DMD. The 130 nm effective pixel size for illumination means that a single pixel illumination could be used for confocal illumination. However, to define patterns on the sample using the DMD the minimum feature size would be 3 DMD pixels corresponding to 390 nm.

For the two camera attached to the DMD illumination system (the ON and OFF paths) the pixel size is effective pixel size if 65 nm. Each pixel is 6.5 μm in size and the optical magnification of the system is 100 \times . For these cameras, the images were binned 2 \times 2 to give effective pixel sizes of 130 nm. The camera mounted at the rear illumination port of the microscope has a pixel size of 13 μm and with the 100X magnification the effective pixel size is 130 nm. The use of effective pixel sizes between 100 and 150 nm for STORM is common. With the PSF of the system being on the order of 300 nm the signal from a single molecule is spread of more several pixels. This allows the PSF to be fitted with a Gaussian function. If the effective pixel size it too big the PSF would be confined to a single pixel and it would be impossible to fit the emission from a single molecule to a Gaussian. If the effective pixel size is to small then the signal from a single molecule is spread over many pixels, although this increases the number of data points the Gaussian can be fitted to it also reduces the signal to noise for each pixel as the number of photos collected per pixel is reduced. It is common in localization microscopy to use effective pixel sizes at or around 100 nm.

The advantage of STORM over confocal microscopy is the increased resolution. However, there are significant disadvantages, these include reduce imaging speed and increased phytotoxicity. Using a DMD based system it should be possible to assign different regions of interest to different imaging modalities. Performing STORM on one area of the sample and confocal [20] or Structured illumination microscopy to another region [21].

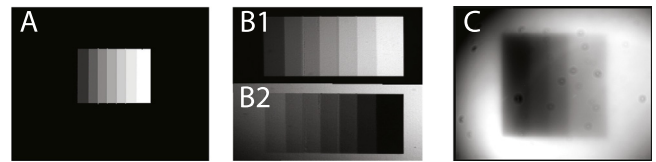


Fig. 2. The ability to deliver controlled power is vital. Part (A) shows the pattern projected on to the DMD, illumination from the ON path. Part (B1 and 2), the image captured by the camera on the ON path (B1) and the OFF path (B2). Part (C) is an image collected by the camera on the backport of the microscope.

3. Discussion

To demonstrate the ability to control power in the system we prepared a coverslip with a thin layer of Alexa 647. This provided a uniform photoluminescence sample which can be used to quantify the patterns projected on to the sample. Fig. 2 shows an 8-bit gradient image, the gradient has value ranges from 0 to 255. Where a 0 represent no power being projected to the sample and 255 represents the full laser power being projected. Values between 0 and 255 represent an amount of time the sample is illuminated, with 127 illuminating the sample for 50% of the time. Part (A) shows the 8-bit image projected on to the sample it consists of a square gradient on a solid black back ground. Parts (B1) and (B2) are the images collected from the ON and OFF paths, the patterns produced are similar to each other. The light collected on the backport part (C) is a direct measurement of the photoluminescence from the sample as shows that the gradient is replicated on the sample. Due to an astigmatism caused by the low pass dichroic filter being used the image has a slight blur. The light collected by the camera on the 'ON' path is sharp and in focus and clearly shows the gradient. It should be noted that light from the sample is also reflected by the DMD so for a DMD pixel set to a value of 127 only half the light from the sample reaches the camera. These images demonstrate one of the disadvantages of the DMD system be used for collection and illumination. With a DMD pixel set to a value of 255 light 100% of the light (ignoring losses) is directed to the microscope and 100% of the light returned from the sample is directed to the camera. However, for a DMD value of 127 50% of the light is directed to the sample, allowing us to lower the illumination but only 50% of the light collected is directed to the ON camera with 50% being sent to the OFF camera. This makes the collection of light from DMD pixels not set to 100% inefficient.

A key goal is not only to control the power delivered to the sample but also the location of that power, specifically for high-resolution applications. To demonstrate the capabilities of the illumination system we imaged NIH 3T3 mouse fibroblast cells expressing the cell adhesion molecule NrCAM [17] through DNA transfection; NrCAM is tagged with an HA epitope recognized by anti-HA antibodies. For STORM imaging a high-power laser as described above is used to project power on to the sample via the DMD, for the data presented in Fig. 3, the DMD was addressed using 1 bit images so the mirrors were either set to 'ON' or 'OFF', i.e. the power delivered to the sample was controlled directly by the laser power rather than the DMD which only controlled to position of the power delivered. Fig. 3(A) and (B) show the images collected by the cameras on the 'ON' and 'OFF' paths respectively. The sample was illuminated using the 'ON' path, for this work a circle and a heart were used for ease of recognition. However, any shape could be used, including masks of single cells or subcellular structures could be. The image contrast settings of the 'ON' and 'OFF' images have been altered to highlight the background in the 'OFF' sample, although only light from the DMD ON pixels should reach the sample there is some scatter which gives a small uniform background. Fig. 3(B) is the summation of 100 collected 'OFF' frames and the area of investigation can be seen showing several 3T3 cells. Illuminated by this scattered light. Because light collected from the sample is also reflected off the DMD, the two illumination areas defined by the heart and circle shapes are completely

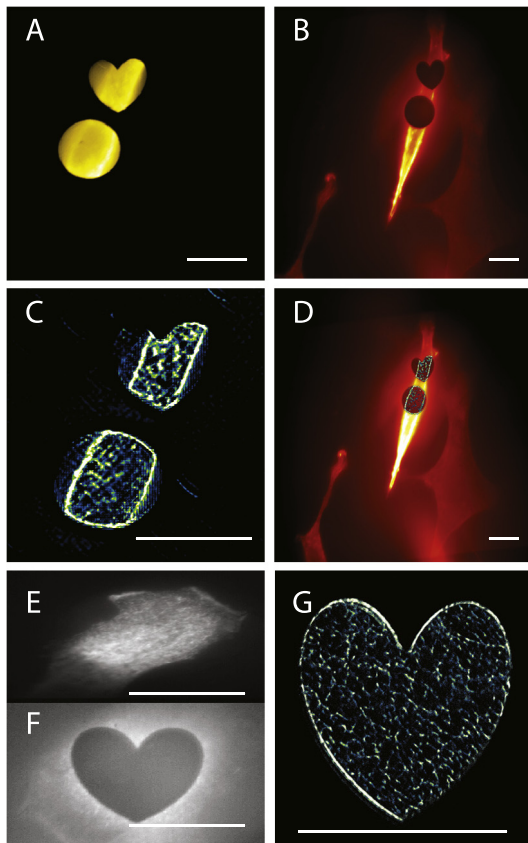


Fig. 3. Part (A), shows a single frame taken before a STORM measurement taken. The image was collected on the ON path with a low intensity illumination source, the same image collected on the OFF channel is shown in part (B). The laser power density is increased to take a STORM data set. After many STORM frames have been collected, the data was reconstructed using SRRF [22], and is given in part (C). Combining parts (A) and (C) gives the part (D). In parts (E–F) a 3T3 cell has been imaged using targeted STORM. Part (E) shows the sample before illumination, part (F) shows the image collected by the OFF channel and part (G) shows the STORM reconstruction of the area. The reconstruction shows the network structure associated with NrCAM. The scale bar in all images is 10 microns.

missing from the camera image because light from the sample at that point cannot reach the camera. The sample was illuminated and 10 k frames were collected, the areas defined showed the characteristic blinking of STORM whereas the areas not defined by the DMD as being ‘ON’ showed no blinking. The frames were analysed using the Super-Resolution Radial Fluctuations (SRRF) algorithm developed by Henriques et al. [22]. The reconstruction from this is given in Fig. 3(C), while Fig. 3(D) shows an overlay of the high-resolution image on the data collected by the ‘OFF’ camera. A larger area of a 3T3 cell is imaged in Fig. 3(E–G), here parts (E) and (F) represent the ‘ON’ and ‘OFF’ respectively, with the image in part (G) showing the reconstructed STORM image. Fig. 3(G) was reconstructed using ThunderSTORM [23], a common ImageJ plugin used for STORM reconstruction.

The STORM images shown in Fig. 3 (C) and (G) show the high-resolution localization of NrCAM molecules inside the targeted area. Structures seen in the images can be attributed to the vesicular transport of NrCAM protein through the cell. We saw a higher concentration of NrCAM near the nucleus which could be the presence of these molecules inside the endoplasmic reticulum, or in the Vesicular network that will carry it to golgi apparatus en route to its normal location at the cell surface. This pattern of expression is typical of cells artificially stimulated to express high levels of exogenous protein after transient DNA transfection. It is worth noting that the reconstructed images show very few localization events from the area outside of excitation area as expected. In both reconstructions, using SRRF and ThunderSTORM,

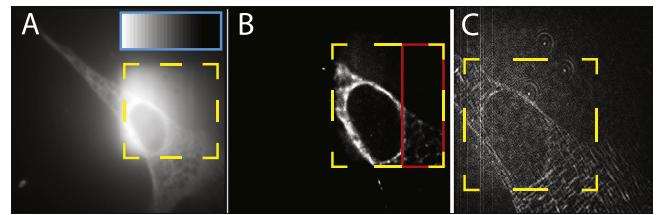


Fig. 4. Part (A) shows a 3T3 cell under illumination from the DMD illumination system, where the power from the system follows a gradient as shown in the inset of part (A). The STORM reconstruction and the SRRF are given in parts (B) and (C) respectively. The yellow box shows the area of excitation. (For interpretation of the references to colour in this figure legend, the reader is referred to the web version of this article.)

the frames of the fields of illumination are classed as structure by the algorithms. This is likely due to the sharp discontinuity of illumination.

Having shown it was possible to deliver enough power to the sample to induce blinking in the sample. The next step is to introduce more control in to the power delivered. It has been shown that several high-resolution adaptive algorithms [SRRF] can deliver different resolutions across an image, which can be dependent on the power delivered to the sample. With higher power densities generally producing higher resolutions. In Fig. 4 we present STORM images which were collected by illuminating the sample with a power density which changes across the sample, this is performed by projecting an 8-bit gradient using the DMD. Fig. 4 (A) shows a 3T3 cell which has been illuminated using the gradient illumination. The gradient is given as an inset to the Fig. 4(A). The square of the sample illuminated using the gradient is highlighted by a yellow box in the figures. To maximize the signal collected from the sample the images were collected using the back port of the microscope, this bypasses the DMD on the return path, but as mentioned above does add a slight astigmatism. The sample was imaged using condition suitable for STORM imaging with the gradient of power applied and ten thousand frames were collected. The resulting frames were analysed using ThunderSTORM Fig. 4(B) and SRRF Fig. 4 (C). The data reconstructed using ThunderSTORM which uses a classic LM approach show a good clear reconstruction for the area of high power illumination. The lower power region as highlighted in red still received power from the laser via the DMD but at a lower intensity, here fewer events are seen at the reconstruction is quite poor. The SRRF reconstruction given in Fig. 4 (C), shows a uniform reconstruction. However, the astigmatism of the system has imparted structure on to the image. SRRF could reconstruct all areas of the sample, including areas which were not directly illuminated. These areas were excited by scattered light within the system. We have used two different reconstruction algorithms, one based on localization microscopy (ThunderSTORM) and one based on radial fluctuations (SRRF). In the data analysed with localization microscopy the change in power across the sample acts in a binary fashion, with regions above a certain power threshold producing single molecule blinking events which can be localized, below this power very few events are localized. For the data analysed using SRRF we obtain a complete image with even regions outside of the illumination pattern having structures defined, this is due to a non infinite contrast ratio of the DMD.

As shown in Fig. 3(B) the sample receives light in areas not intended to be illuminated. Although this level of light is low it is still undesirable, to investigate the effect of stray light at the illumination powers used in STORM we took low illumination light intensity images before and after the storm imaging. Fig. 5(A–C) shows a 3T3 sample used in this work, A is the cell taken before imaging taken with the ON channels at low light levels, B is taken during the STORM imaging using the OFF camera, C is the same cell imaged after STORM imaging. Part D, shows the average signal level taken from two small areas of the sample taken during 50 frames of imaging. The blue line represents an area of the sample targeted to be illuminated (defined as ON) and the red from an

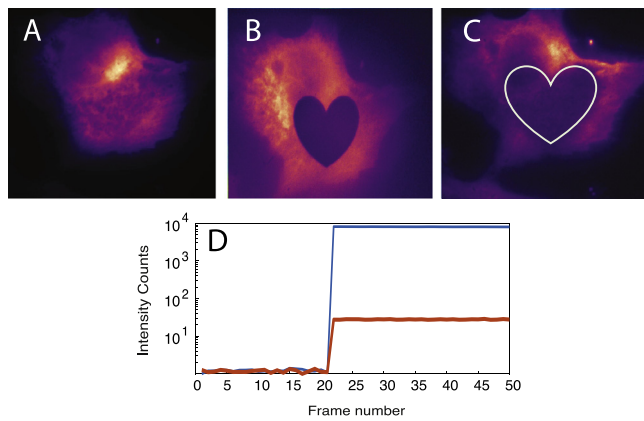


Fig. 5. A 3T3 cell is imaged using STORM, part A shows the sample illuminated under low power. The sample is illuminated under high power using a heart shape pattern, a single frame from the OFF camera is given in part B. After 10 k frames of high illumination the sample was again re-imaged using low power this is given in part C. Finally, part D shows the average intensity from a region of the sample during illumination for an ON region (BLUE) and OFF region (RED), showing that even the OFF regions are illuminated. (For interpretation of the references to colour in this figure legend, the reader is referred to the web version of this article.)

area not targeted (defined as OFF). In the first 20 frames, there is no laser illumination, the laser is turned on at the 20th frame. It can be seen in the log plot that light from the laser is reaching the regions of the sample defined as OFF. The ratio between the OFF and ON intensities is on the order of 300. In this work, we apply about 0.5 mW of power per ON pixel to the sample, the equivalent power supplied for an OFF pixel is therefore roughly 2 μ W.

4. Conclusion

The ability to target laser power to a sample with diffraction limited resolution can be used to selectively target areas of a sample for high-resolution imaging without damaging other areas of the sample. The application of DMD technology to STORM does not increase the speed of acquisition. It does allow the selection of specific regions of interest within the field of view, allowing us to isolate specific regions of the sample in space and time for study through STORM without damaging the rest of the sample through high illumination powers. However, it should be possible to apply techniques which measure the resolution of the image such as Fourier ring correlation (FRC) as described by Nieuwenhuizen et al. [24] to the area targeted and stop imaging when a maximum resolution (or required) resolution is achieved. This may require different amounts of time across the image, depending on the sample geometry as discussed by Fox-Roberts et al. [25].

It has been shown that the resolutions obtainable with SRRF are power dependent [22]. As such applying different power densities to different areas of the sample, could in the future, be used in conjunction with algorithms such as SRRF to sacrifice the imaging resolution against power. In this work, we were unable to quantify the direct relationship between power and resolution for SRRF.

Acknowledgements

This work was supported by the Sheffield University's 'Imagine: Imaging Life, a 2022 futures initiative. We would like to thank Cairn-Research for their help in this project.

References

- [1] Eugene Hecht, *Optics*, fifth ed., Pearson Education, 2016.
- [2] M.G.L. Gustafsson, Surpassing the lateral resolution limit by a factor of two using structured illumination microscopy, *J. Microsc.* 198 (2000) 82–87.
- [3] M. Gustafsson, Nonlinear structured-illumination microscopy: wide-field fluorescence imaging with theoretically unlimited resolution, *Proc. Natl. Acad. Sci. USA* 102 (2005) 13081–13086.
- [4] T.A. Klar, S. Jakobs, M. Dyba, A. Egner, S.W. Hell, Fluorescence microscopy with diffraction resolution barrier broken by stimulated emission, *Proc. Natl. Acad. Sci. USA* 97 (2000) 8206–8210.
- [5] M.J. Rust, M. Bates, X. Zhuang, Sub-diffraction-limit imaging by stochastic optical reconstruction microscopy (STORM), *Nat. Methods* 3 (2006) 793–795.
- [6] E. Betzig, G.H. Patterson, R. Sougrat, O.W. Lindwasser, S. Olenych, J.S. Bonifacino, M.W. Davidson, J. Lippincott-Schwartz, H.F. Hess, Imaging intracellular fluorescent proteins at nanometer resolution, *Science* 313 (2006) 1642–1645.
- [7] S.T. Hess, T.P.K. Girirajan, M.D. Mason, Ultra-high resolution imaging by fluorescence photoactivation localization microscopy, *Biophys. J.* 91 (2006) 4258–4272.
- [8] S.A. Jones, S.-H. Shim, J. He, X. Zhuang, Fast, three-dimensional super-resolution imaging of live cells, *Nat. Methods* 8 (2011) 499–508.
- [9] Sina Wäldchen, et al., Light-induced cell damage in live-cell super-resolution microscopy, *Sci. Rep.* 5 (2015) Article number: 15348.
- [10] S.J. Holden, et al., High throughput 3D super-resolution microscopy reveals *Caulobacter crescentus* in vivo Z-ring organization, *Proc. Natl. Acad. Sci.* 111 (2014) 4566–4571.
- [11] Guy.M. Huygen, et al., Biological applications of an LCoS-based programmable array microscope (PAM), *SPIE Proc.* 6441 (2007).
- [12] Dan Dan, et al., DMD-based LED-illumination Super-resolution and optical sectioning microscopy, *Sci. Rep.* 3 (2013) Article number: 1116.
- [13] R. Heintzmann, et al., A dual path programmable array microscope (PAM): simultaneous acquisition of conjugate and non-conjugate images, *J. Microsc.* 204 (2001) 119–137.
- [14] Texas Instruments, <http://www.ti.com/product/DLP7000>.
- [15] Vialux Germany, <https://www.vialux.de/en/superspeed-v-modules.html>.
- [16] MathWorks, <https://uk.mathworks.com>.
- [17] Davey, et al., Synapse associated protein 102 is a novel binding partner to the cytoplasmic terminus of neurone-glia related cell adhesion molecule, *J. Neurochem.* 94 (5) (2005) 1243–1253.
- [18] Dang, et al., TAG1 regulates the endocytic trafficking and signaling of the semaphorin3A receptor complex, *J. Neurosci.* 32 (30) (2012) 10370–10382.
- [19] Graham T. Dempsey, et al., Evaluation of fluorophores for optimal performance in localization-based super-resolution imaging, *Nat. Methods* 8 (2011) 1027–1036.
- [20] Hanley Verwee, van VlietJovin Verbeek, Theory of confocal fluorescence imaging in the programmable array microscope (PAM), *J. Microsc.* 189 (1998) 192–198.
- [21] D. Dan, et al., DMD-based LED-illumination super-resolution and optical sectioning microscopy, *Sci. Rep.* 3 (2013) 1116.
- [22] N. Gustafsson, et al., Fast live-cell conventional fluorophore nanoscopy with ImageJ through super-resolution radial fluctuations, *Nature Commun.* 7 (2016) 12471.
- [23] M. Ovesný, P. Křížek, J. Borkovec, Z. Švindrych, G.M. Hagen, ThunderSTORM: a comprehensive ImageJ plugin for PALM and STORM data analysis and super-resolution imaging, *Bioinformatics* 30 (16) (2014) 2389–2390.
- [24] R.P.J. Nieuwenhuizen, et al., Measuring image resolution in optical nanoscopy, *Nat. Methods* 10 (2013) 557–562.
- [25] P. Fox-Roberts, et al., Local dimensionality determines imaging speed in localization microscopy, *Nature Commun.* 8 (2017) 1–10.